N 71 11457

NASA TECHNICAL MEMORANDUM

NASA TM X-52917

NASA TM X-52917

CASE FILE COPY

EXPERIMENTAL ANALYSIS OF THE FITZGERALD APPARATUS

by James P. Cusick and Donald R. Behrendt
Lewis Research Center
Cleveland, Ohio

EXPERIMENTAL ANALYSIS OF THE FITZGERALD APPARATUS

by James P. Cusick and Donald R. Behrendt

National Aeronautics and Space Administration
Lewis Research Center
Cleveland, Ohio

SUMMARY

Experimental measurements on the dynamic compliance machine developed by E. R. Fitzgerald are presented to demonstrate that the anomalous modes associated with Fitzgerald's results are a consequence of large non-ideal drive tube motions. The drive tube designed by Fitzgerald is modified to permit external insertion or removal of a shorted turn similar to the one inherent in the original design. Experimental data is taken with and without the shorted turn on the drive tube. The sample compliance values computed from this data show that the shorted turn is responsible for the anomalous loss compliance values reported by Fitzgerald.

E-6024

INTRODUCTION

Fitzgerald (refs. 1 and 2) describes an apparatus which he uses to investigate the mechanical properties of solids by measurement of the dynamic shear compliance. The apparatus shown in figure 1 subjects a pair of samples to two mechanical forces: (1) a sinusoidal shearing force of preselected frequency which is applied by means of an aluminum drive tube, and (2) a static compressive force which clamps the samples to both the drive tube and the inertial floating mass. The static clamping force is developed by a screw-driven wedge in the floating mass assembly (see fig. 1). The alternating force is developed by an alternating current flow in coils 1A and 2A; the coils being situated in a radial magnetic field.

Fitzgerald determines the mechanical compliance of the sample by measurement of the electrical impedance of a coil 2A; coil 2A forms on an element of an impedance bridge circuit (refs. 1 and 2). The measured electrical impedance of the coil of wire is altered by the induced voltages that arise from the velocity of the drive tube. In references 1 and 2, Fitzgerald shows how this electrical impedance is measured and how it is related to the mechanical impedance of the moving system.

The mechanical impedance thus obtained by Fitzgerald combines the mechanical impedances of the drive tube, the floating mass, and the samples. In order to determine the mechanical impedances of the samples alone, Fitzgerald resorts to a vector subtraction of mechanical impedances based upon his own mechanical model of the machine. This method requires knowledge of the mechanical impedance of the machine in three basic configurations: (1) the free tube impedance obtained with nothing attached to the drive tube; (2) the clamped tube impedance obtained with the floating mass and drive tube clamped directly together with samples, and

(3) the clamped sample impedance (i.e., the mechanical impedance of the system with the drive tube, samples and floating mass all clamped together). These mechanical impedances are determined experimentally; the first two comprise the so-called calibration data for the machine.

The sample mechanical impedance deduced by Fitzgerald is reported in the form of a dynamic shear compliance spectrum in which the vector compliance is plotted against frequency and is resolved into two components: the first component, designated J', is proportional to the energy stored and recovered in one cycle of the shearing motion; the second component, designated J'', is proportional to the energy dissipated in a cycle. The frequency range of the machine is nominally 50 to 5000 Hz.

The shear compliance spectra reported by Fitzgerald (refs. 3 to 7) and Gotsky and Stearns (ref. 8) for hard crystalline samples show marked differences from compliance values deduced from elastic theory. The three principal differences are as follows:

(1) A low frequency (50 to 500 Hz) in-phase compliance value, which is much larger than elastic theory prediction, suggests that the sample is softer than elastic predictions.

(2) Several resonances appear in the compliance spectra which are both unexpected and unexplained.

(3) The quadrature component of the compliance (J'') near large high-frequency resonances (about 3000 Hz) is asymmetric about the resonance frequency and is sometimes negative immediately above the resonance frequency. Fitzgerald states that the negative sample damping implied by a negative loss compliance is the result of a process internal to the sample.

In references 1 and 2, Fitzgerald presents his analysis of the machine. The assumptions contained in that analysis which are pertinent to this report are as follows:

(1) The four sample surfaces which contact the machine (i.e., contact the drive tube and the floating mass) connect with the machine in such a manner as to provide atom-to-atom contact between sample and machine.

(2) The floating mass assembly behaves as rigid mass at all frequencies of measurement.

(3) The samples, drive tube, and floating mass are always in perfect alignment.

(4) The motion of the drive tube is uniaxial and only two ideal machine modes exist; namely, the axial modes produced by the tube mass resonating with the restoring force constant provided by either the suspension system or the sample.

Fitzgerald's analysis makes no provision for nonideal machine performance. As a consequence the subtraction method for determining sample properties allows a nonideal machine mode to be interpreted as a sample effect.

The present authors[9] have presented a mechanical model of the machine that describes several nonideal modes which must exist at some frequency. These nonideal modes could account for all resonance anomalies reported by Fitzgerald.

In another report[10] the Fitzgerald machine is analyzed to take into account the shorted turn on the drive tube designed by Fitzgerald (see fig 1). The equations derived reproduce the anomalies in Fitzgerald's calibration and sample loss compliance data.

The purpose of this report is to demonstrate by direct measurement that 1) the drive tube of the Fitzgerald machine executes large non-ideal motion at each anomalous resonance observed in the frequency range of the machine (50 to 5000 He) and 2) the shorted turn on the drive tube is the only source of the anomalous calibration and negative loss compliance effects reported by Fitzgerald.

EXPERIMENTAL RESULTS

Three different experimental measurements are reported, in the following order 1) Measurement of the drive tube velocity by means of the pick-up coil 2A; 2) Measurement of non-axial tube motion by means of a capacitance probe technique and; 3) Measurements of the drive tube motion (both axial and radial) with and without a shorted turn on the drive tube.

(1) Drive Tube Velocity as Measured by Coil 2A

In order to measure the drive tube velocity as seen by coil 2A (see fig 1) the voltage generated in coil 2A is fed to a AC to DC logarithmic converter with suitable passband and the DC voltage produced is fed to the Y axis of an X-Y recorder. The Y axis deflection is thus proportional to the logarithm of the AC signal amplitude. The X-axis of the X-Y plotter is driven by a DC voltage of a potentiometer which is mechanically coupled to the frequency control of a Beat frequency oscillator. A small clock motor drives the oscillator through the desired range of 20 to 20 khz at a rate of 20 sec per frequency decade. For these measurements the current in coil 2B (see fig 1) is adjusted to provide a mutual inductance balance at 2500 hz, by the balance method employed by Fitzgerald.

Results

Figure 2 is a typical plot of the logarithm of the voltage in coil 2A vs excitation frequency for a free drive tube. The velocity maxima occurs near 20 hz corresponding to the free tube resonance frequency. In the range of 300 to 700 hz perturbations in drive tube velocity occur corresponding

to resonant modes of the drive tube support wires. A complex resonance

effect in the 12 to 20 khz region is due to either drive tube or shielding

coil modes. This resonance is above the frequency range of interest of

this report.

Figure 3 is a velocity plot of the clamped tube configuration where

the drive tube is clamped to the floating mass without samples. The higher

noise level evident in this plot is a result of the lower velocity (i.e.,

lower signal voltage in coil 2A). The expected resonant frequency for

this configuration (about 1.2 hz) is not shown due to low frequency limita-

tions of the recording technique. Several prominent resonances occur in the

clamped tube configuration.

Two sodium chloride samples .62x3.1 cm and .30 cm thick were installed

in the Fitzgerald machine with the 3.1 cm direction parallel to the shear

direction, and lightly clamped to the drive tube and floating mass. The

velocity plot resulting is shown in figure 4. The large velocity near 1000 hz

is the expected resonance brought about by the sample stiffness and the drive

tube mass. Another resonance is expected near 1.2 hz for the rigid body

motion of drive tube mass and floating mass together with the restoring

force constant of the wire suspension system. The negative slope of the

velocity data near 100 hz is due to this mode. Since this latter mode lies

below the frequency range of interest in this report it will not be discussed

further. The former mode will be referred to as the "system resonance" mode.

It should be noted that the higher velocity in the low kilohertz

region brought about by the system resonance provides greater mechanical

energy to excite machine modes in this frequency region. Several such

resonances are seen in the envelope of the system resonance mode.

Increasing static clamping force on the samples results in greater area

of contact between samples and machine surfaces and thereby raises the ef-

fective stiffness of the samples to the shearing motion of the drive tube.

Figures 5 and 6 show the effect of increasing static clamping force on the

system resonance frequency. The increase in magnitude of the extaneous

resonances becomes so large in the latter figure that the system resonant

frequency cannot be determined by visual inspection alone. The sample

dimensions and orientation in the machine for figures 4 thru 6 corresponds

to the situation reported by Gotsky and Stearns[8] in which for light clamp-

ing forces they observe a large compliance resonance near 600 hz. Figure 5

shows a prominent resonance in the drive tube velocity in this frequency

region.

If the sample crossection is approximately square (.61 cm on a side and

.30 cm thick) and oriented with an edge of the square face parallel to the

shear direction different extraneous resonances result. In these experiments

a strain gage mounted on the drive tube was used to measure clamping force.

For very small static clamping force (4.7×10^5 dynes) the velocity plot

given in figure 7 results. Increasing clamping force to (11.1×10^5 dynes)

produces the velocity plot of figure 8. Increasing clamping force to(44.4×10^5

dynes) yields a velocity plot as shown in fig 9. The system resonance

frequency in figure 9 is expected to be above 20 khz by elastic compliance

considerations. It is seen from fig 9 that extraneous modes persist in the

3 to 10 kilohertz region. A particular mode with this property is the non-

rigid floating mass mode discussed in detail in reference 9. (See figures

3 and 8 of reference 9.)

(2) Measurement of Nonaxial Tube Motion

The analysis of the Fitzgerald apparatus given in reference 1 assumes

that the drive tube is constrained to move only in the axial direction

Extraneous resonant modes which produce nonaxial drive tube motion will

perturb the axial tube motion and produce an apparent resonance in the drive

tube as seen by coil 2A. In order to observe nonaxial tube motion, a

capacitive probe system is employed which measures nonaxial drive tube dis-

placement. A drawing of the capacitive probe is shown in fig 10. The non-

axial displacement of the drive tube produces a voltage change in the

capacitive probe. This voltage is amplified by an A.C. amplifier with

suitable pass band and high input impedance (10 megohm). The output of the

amplifier is fed to a tracking filter which produces a narrow pass band at

the drive tube excitation frequency. The output of the tracking filter is

fed to the log AC/DC converter and plotted as the Y axis of the X-Y recorder.

The nonaxial tube motion is correlated with drive tube resonances as

seen by coil 2A by comparing X-Y plotter displays. The X-Y plotting pre-

sents frequency as the X axis and both the drive tube velocity (as seen

by coil 2A) and the capacitor probe output as the Y-axis.

Such a comparison for the free drive tube is shown in figure 11; the left and bottom capacitor probes and coil 2A are shown. Each capacitor probe shows large nonaxial motions at the drive tube support wire resonances. A small contribution of axial tube motion is present in each capacitor probe output. This arises from stray capacitance between the drive tube and the aluminum foil of the capacitor probe. This stray capacitance is in the axial direction so that axial tube displacement causes a change in the stray capacitance and a capacitor probe voltage results.

In figure 12 a comparison is presented of drive tube velocity as measured by coil 2A and capacitor probe outputs for left, right and bottom. These data are obtained with a NaCl sample clamped between the drive tube and floating mass with moderate force (8.8×10^5 dynes). The frequency range shown is 1000 to 10,000 hz. The capacitor data show large displacement variations at the extraneous drive tube velocity modes.

(3) Shorted Turn Effects

The drive tube designed by Fitzgerald has an aluminum extension concentric with coil 1A, which lies in the radial magnetic field (see fig 1). This

metalic extension is called the shorted turn. The current in coil 1A pro-
duces about 90% of the sinusoldal force applied to the drive tube. Mutual
inductance between coil 1A and the shorted turn as well as motion of the
shorted turn in the magnetic field, induce currents in the shorted turn.
The induced currents result in an additional force on the drive tube which
is, in general, out of phase with the force produced by the current in coil
1A.

Fitzgerald's analysis[1] of the machine does not consider the effect of
the shorted turn. The analysis of Behrendt and Cusick[10] includes shorted
turn effects and yields equations which predict the negative damping re-
ported by Fitzgerald for both sample data and machine calibration data.

In order to demonstrate that the damping anomalies reported with the
Fitzgerald machine are due to shorted turn effects it is necessary to perform
calibration and sample measurements with and without the shorted turn. It
should be noted that the shorted turn cannot be removed by simply splitting
the aluminum section of the drive tube since such a procedure will only
slightly modify the induced currents.

Drive Tube Modification

The shorted turn extension of Fitzgerald's drive tube was machined off and a fiberglass-epoxy extension section was fabricated and cemented to the remaining portion of the drive tube (see fig 13). Two slots were machined in the fiberglass extension to receive the pickup coil (2A) and the drive coil 1A. Before winding coil 1A on the tube extension, sixty turns of #26 insulated copper wire were wound in the coil 1A position. The ends of this 2-layer winding (called coil 1C) were brought out so that the coil ends could be left disconnected or soldered together simulating the shorted turn of Fitzgerald's design. Coil 1A was then wound directly above coil 1C. The total mass of the modified drive tube, coils and support wires is 68.1 grams.

The modified drive tube shows extraneous modes and nonaxial motion very similar to the original Fitzgerald drive tube. The drive tube velocity plot data is altered by the presence of a shorted turn on the drive tube. This can be observed by comparing velocity plot data for two cases, (1) coil 1C open circuited and (2) coil 1C close circuited. For coil 1C close-circuited the principle effects are (a) a decrease in the drive tube velocity near the free tube resonance ($\sim$ 16 hz) and (b) suppression of small motional

instabilities in the low kilohertz region. Figure 14 presents a velocity

plot of the free (unclamped) drive tube, with the coil 1C close-circuited

(i.e. with a shorted turn) and open circuited (i.e., without a shorted turn).

Closing coil 1C appears to have no appreciable effect on extraneous

mode effects as measured by coil 2A. Figure 15 compares both velocity plots

for a pair of sodium chloride samples clamped in the machine. The slight

change in peak frequency for the large maxima and minimum are probably not

significant. The shorted turn appears to damp-out small instabilities in the

low kilohertz region.

The capacitance probes indicate that some nonaxial modes are affected

by close-circuiting coil 1C while other modes appear to be unaltered.

Figure 16 shows a drive tube velocity plot as measured with coil 2A for a

pair of clamped sodium chloride samples. Also shown is the output of the

left and right capacitor probes for both close-circuit and open-circuit coil

1C configurations. The left capacitor probe shows little sensitivity to the

presence of a closed circuit in coil 1C, the right capacitor probe shows a

large reduction in nonaxial amplitude when coil 1C is close-circuited.

A close-circuited coil 1C should have a profound effect upon the mechanical impedance calculated by Fitzgerald's method. The damping component of the mechanical impedance of a free drive tube is designated G_{12}^O in Fitzgerald's analysis.[1] Figure 17 presents values of G_{12}^O calculated from calibration data for Fitzgerald's drive tube before modification. The negative values of damping evident above 1000 hz can be explained in terms of the shorted turn analysis of reference 10. The curve thru the data is calculated from equation 23 of reference 10 for a shorted turn parameter value 1.667×10^{-5} sec. This parameter is the ratio of inductance to resistance of the shorted turn.

In order to ascertain that all negative damping effects are due to the shorted turn, G_{12}^O was calculated from calibration data taken for the modified drive tube with coil 1C open-circuited as well as close-circuited. The results are compared in figure 18. For frequencies above 600 hz the close circuit data produces negative values of G_{12}^O. The larger shorted turn parameter and increased tube mass associated with coil 1C compared with the original Fitzgerald shorted turn results in a steeper fall off with frequency in agreement with equation 23.[10]

For all data with coil 1C open-circuited G_{12}^O is positive. The effect

of drive tube resonances and motional instabilities discussed above, combine

to produce considerable scatter above 2000 hz.

The effect of the shorted turn on resonances in sample compliance data

as calculated by Fitzgerald is shown in figure 19. Two sodium chloride

samples are clamped in the machine and compliance values are calculated form

data taken with the coil 1C open-circuited and with coil 1C close-circuited.

The loss compliance $(J")$ is shown in fig 19. The close-circuited data re-

sult in calculated values for loss compliance which are negative on the

high frequency side of a resonance. The loss compliance curve is also non-

symmetric about the resonance frequency. Compliance values calculated from

data obtained with coil 1C open-circuited yield a symmetric curve with no

negative values of compliance.

The shorted turn analysis of reference 10 predicts a mixing of both

components of sample compliance. This mixing produces the asymmetry seen

in fig 19. The storage compliance (J') corresponding to the data presented

in fig 19 is compared in figure 20. The expected assymetry is not obvious

from this comparison due to the discrete frequency nature of the data taking

process. At the time of data collection, the frequency of compliance extremum

is not known, thus a convenient frequency increment is used. This process

does not give good resolution of compliance extremum values.

Discussion

The storage compliance values reported by Fitzgerald[3,4,5,6] at fre-

quencies removed from resonant effects (about 500 cps) are systematically

higher (by up to a factor of 100) than values deduced from elastic constants.

This error arises from the assumption of Fitzgerald's analysis that total

sample surface area is in contact with the machine surface. This assumption

denies the existence of surface irregularities and roughness.

The change in system resonant frequency with static clamping shown in

figures 4 thru 9 is a graphic display of increasing sample stiffness by

increasing area of contact between samples and machine.

Fitzgerald has fit several anomalous resonances by a simple analytic

resonator function. The coefficient of the acceleration term[5-7] is found

to be several hundred times larger than the sample mass. This is expected if

the resonances are caused by nonideal motion of the drive tube on nonrigid

motion of the floating mass assembly, since large perturbations in drive

tube motion can only result from a resonating body with a mass about equal

to or greater than the drive tube mass. In reference 9 several possible

nonideal modes are analyzed which satisfy this requirement. In that refer-

ence the effect of these modes upon Fitzgerald's compliance data is also

shown.

Conclusions

The data presented above shows that the Fitzgerald machine has an

abundance of extraneous modes which are observable in the drive tube velocity

plots. Associated with each of these modes is a large nonaxial displacement

of the drive tube. Since nonaxial tube motion is not considered in

Fitzgerald's analysis we must conclude that the resonant effects reported

by Fitzgerald and attributed by him to the sample under test are not in fact

produced by an intrinsic property of the latter.

The shorted turn data presented above shows that the analysis of

Behrendt and Cusick[10] is essentially correct in explaining the frequency

dependence of the calibration data G_{12}^O and the negative loss compliance

anomalies. We thus conclude that these effects are due to the shorted turn

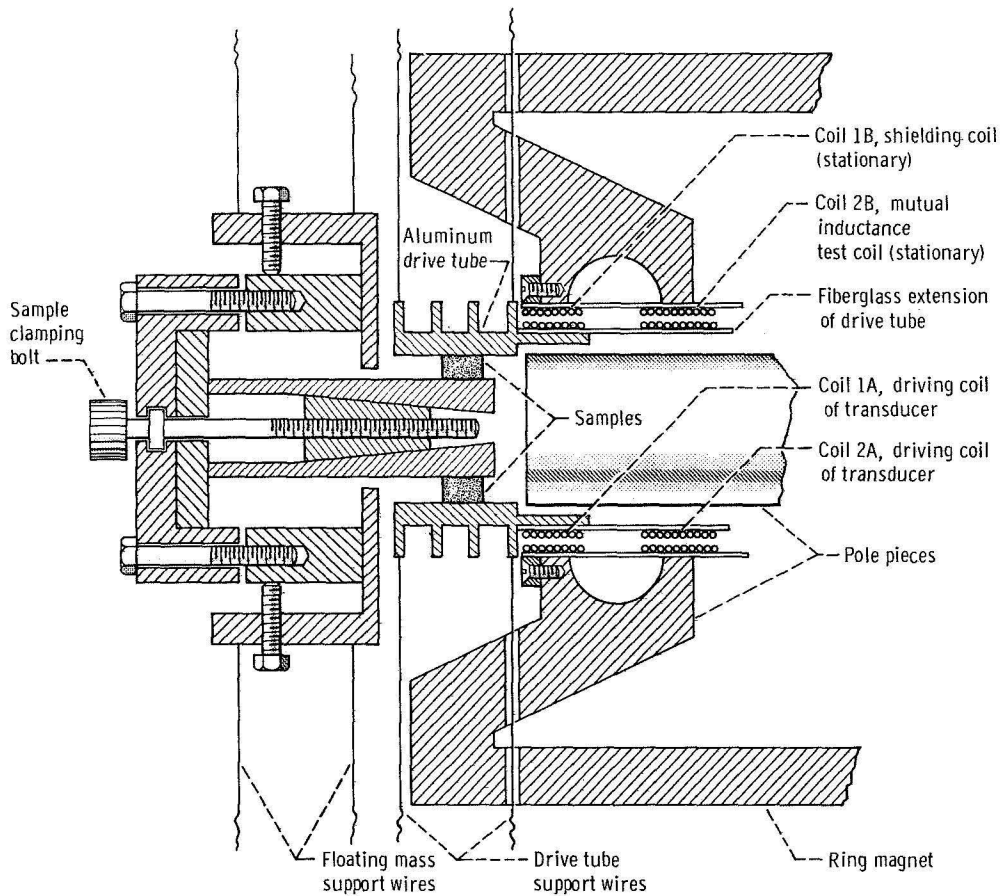and do not reflect intrinsic material properties of the samples.

Finally, the anomalously large low-frequency compliance reported by

Fitzgerald for all crystalline materials tested is shown to be a result of

the assumption that sample-to-mechine contact is independent of clamping

force. We conclude that Fitzgerald's results do not constitute a valid deter-

mination of dynamic compliances.

REFERENCES

1. Fitzgerald, Edwin R.; and Ferry, John D.: Method for Determining the

Dynamic Mechanical Behavior of Gels and Solids at Audiofrequencies;

Comparison of Mechanical and Electrical Properties. J. Colloid Sci.,

vol. 8, 1953, pp. 1-34.

2. Fitzgerald, Edwin R.; Dynamic Electrical and Mechanical Behavior of

Polymeric Systems. Ph.D. Thesis, Univ. Wisconsin, 1951.

3. Fitzgerald, Edwin R.: Mechanical Resonance Dispersion of Metals at

Audio-Frequencies. Phys. Rev., vol. 108, no. 3, Nov. 1, 1957,

pp. 690-706.

4. Fitzgerald, Edwin R.: Yield Strength of Crystalline Solids from

Dynamic Mechanical Measurements. Developments in Mechanics.

Vol. 1. J. E. Lay and L. E. Malvern, eds., Plenum Press, 1961,

pp. 10-38.

5. Fitzgerald, Edwin R.: Mechanical Resonance Dispersion in Single

Crystals. Phys. Rev., vol. 112, no. 4, Nov. 15, 1958, pp. 1063-

1075.

6. Fitzgerald, Edwin R.: Mechanical Resonance Dispersion and Plastic

Flow in Crystalline Solids. J. Acoust. Soc. Am., vol. 32, no. 10,

Oct. 1960, pp. 1270-1289.

7. Fitzgerald, Edwin R.: Mechanical Resonance Dispersion in Quartz at

Audio-Frequencies. Phys. Rev., vol. 112, no. 3, Nov. 1, 1958,

pp. 765-784.

8. Gotsky, Edward R.; and Stearns, Carl A.: Mechanical Resonance Dis-

persion and Stress-Strain Behavior of Several Ionic Single Crystals.

NASA TN D-2566, 1965.

9. Cusick, James P.; and Behrendt, Donald R.: Resonant Mode Analysis of

the Fitzgerald Apparatus. NASA TN D-5103, 1969.

10. Behrendt, Donald R.; and Cusick, James P.: Mathematical Analysis of

the Fitzgerald Apparatus. NASA TN D-5116, 1969.

Coil 1B, shielding coil (stationary)

Coil 2B, mutual inductance test coil (stationary)

Fiberglass extension of drive tube

Coil 1A, driving coil of transducer

Coil 2A, driving coil of transducer

Pole pieces

Ring magnet

Aluminum drive tube

Sample clamping bolt

Samples

Floating mass support wires

Drive tube support wires

CD-10255-23

Figure 1. – Simplified view of Fitzgerald apparatus. Note portion of aluminum drive tube that extends into magnetic field.
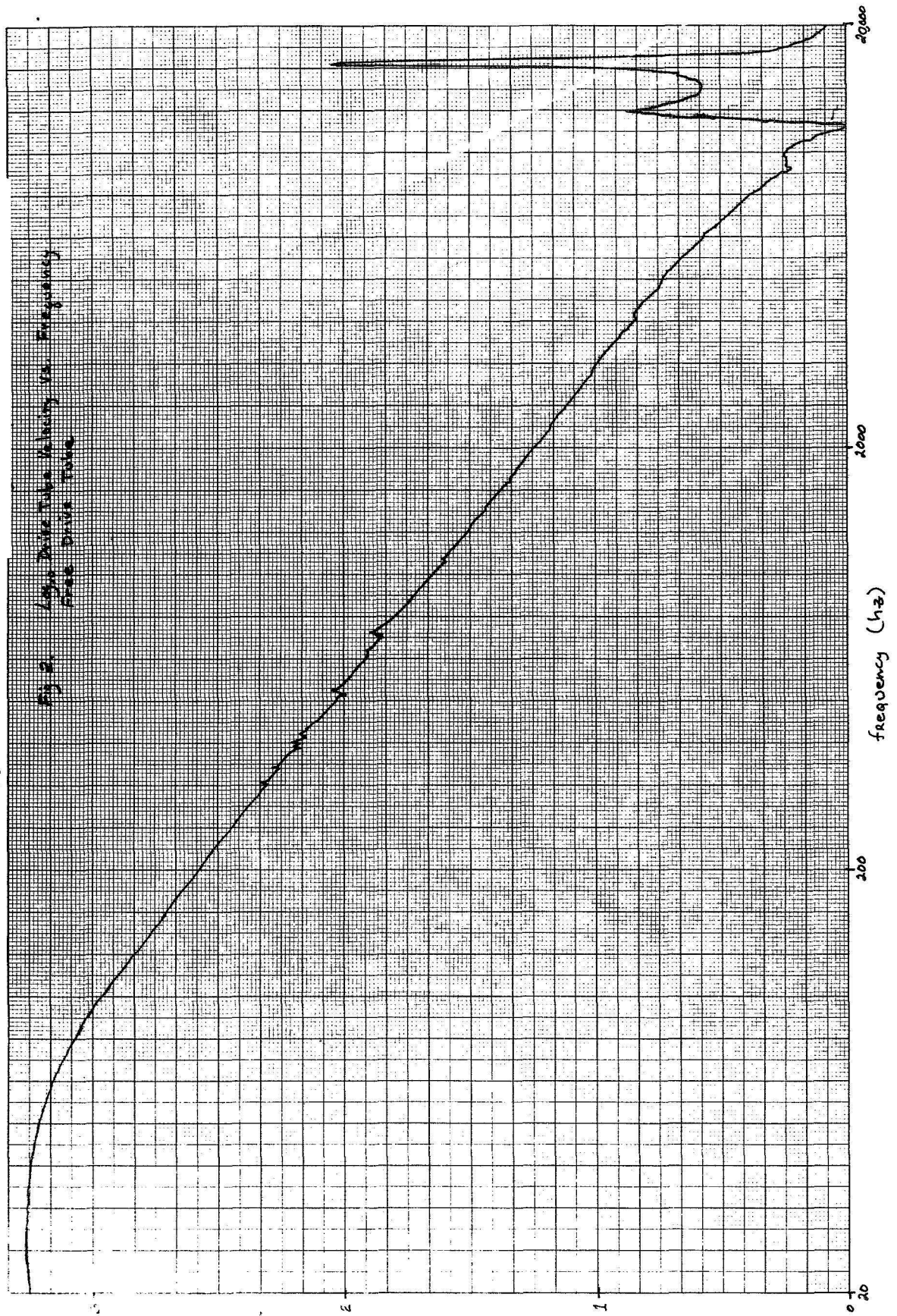
Fig 2. Log_{10} Drive Tube Velocity vs. Frequency
Free Drive Tube
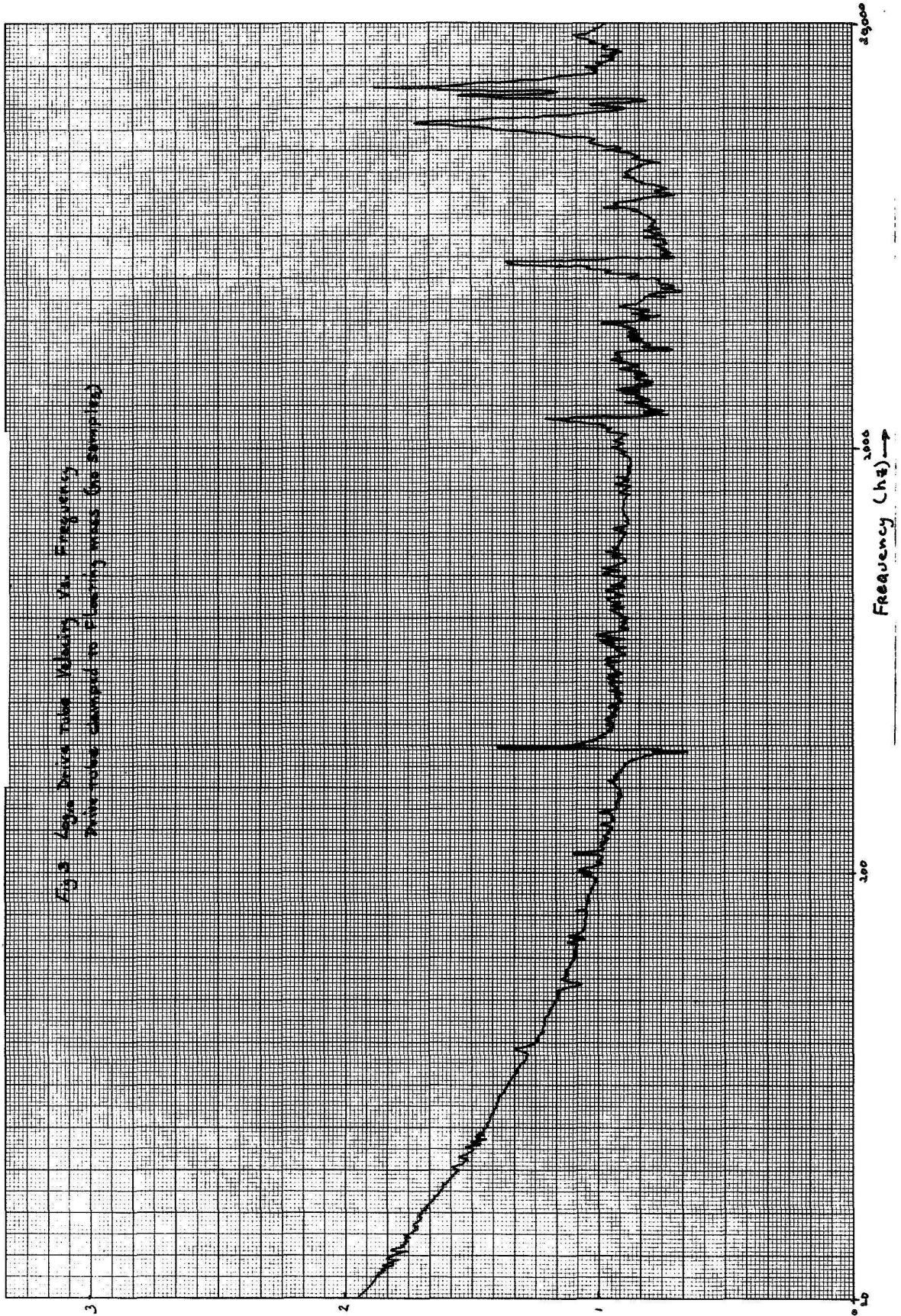
Frequency (Hz)

Log_{10} Drive Tube Velocity

20   200   2000   20,000

Fig. 3 6.3.5 Drive Tube Velocity Vs. Frequency

Fourteenth octave smoothing (to octave frequency window (no sampling)
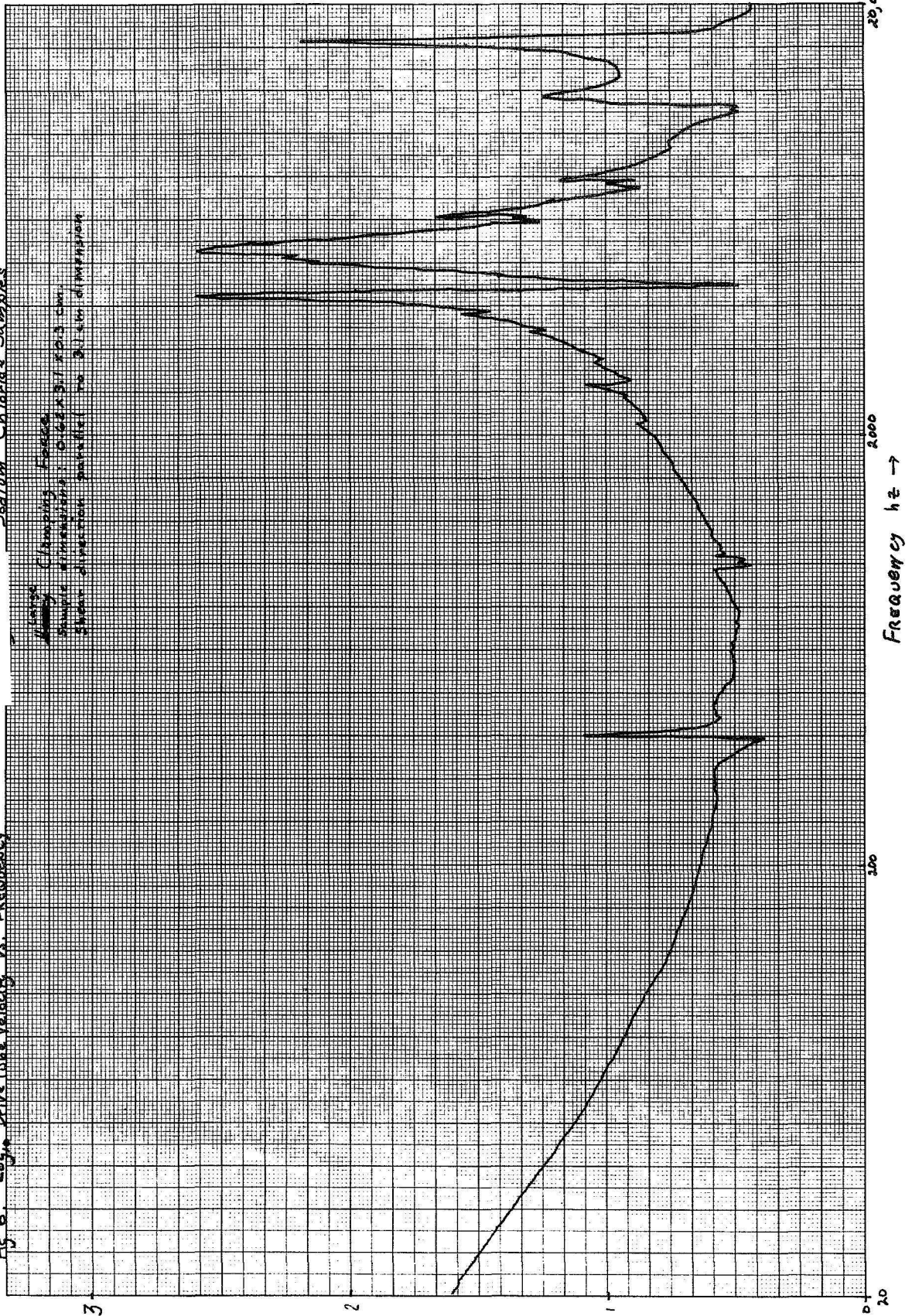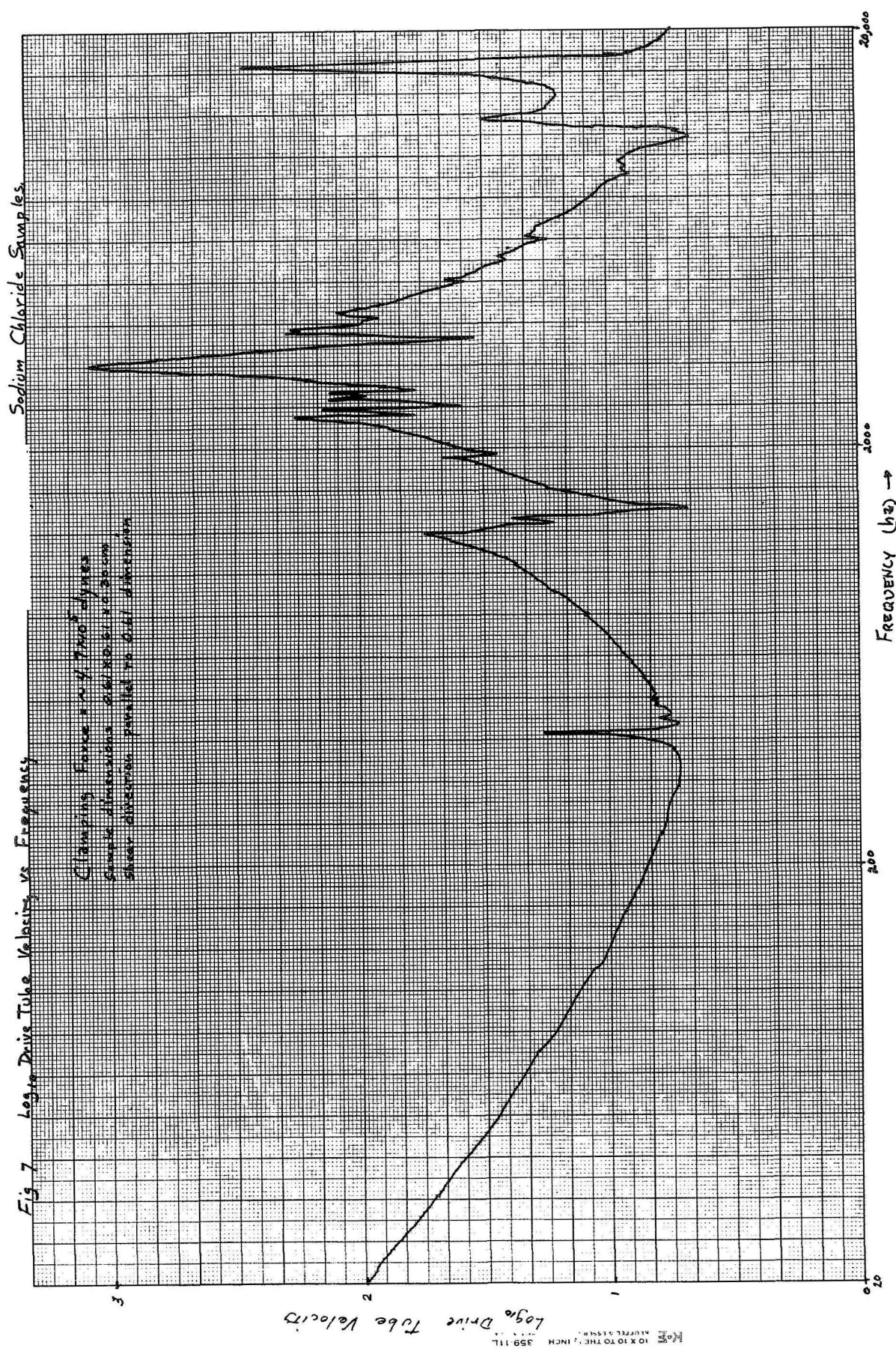
Frequency (hz) →

Log₁₀ Drive Tube Velocity

Fig. 4 Log₁₀ Drive Tube Velocity vs Frequency

Sodium Chloride Samples Small Clamping Force

Sample dimensions .625 x 3.14 x 30 cm
Shear direction parallel to 3/4 cm dimension...

FREQUENCY (Hz) →

Log₁₀ Drive Tube Velocity

Fig 5. $\log_{10}$ Drive Tube Velocity vs Frequency

Sodium Chloride Samples

Moderate Clamping Force
Sample dimensions : 4.2 x 3.1 x 0.3 cm
Shear direction parallel to 3.1 cm dimension

$\log_{10}$ Drive Tube Velocity

3

2

1

Frequency (hz) →

20   200   2000   20,000

Fig. 6. Log₁₀ Drive Tube Velocity vs. Frequency

Sodium Chloride Samples

Fig 7   Legto Drive Tube Velocity vs Frequency   Sodium Chloride Samples.

Clamping Force and 7x10⁵ dynes
Sample dimensions .61x1.2x2.35 cm
Shear direction parallel to first dimension
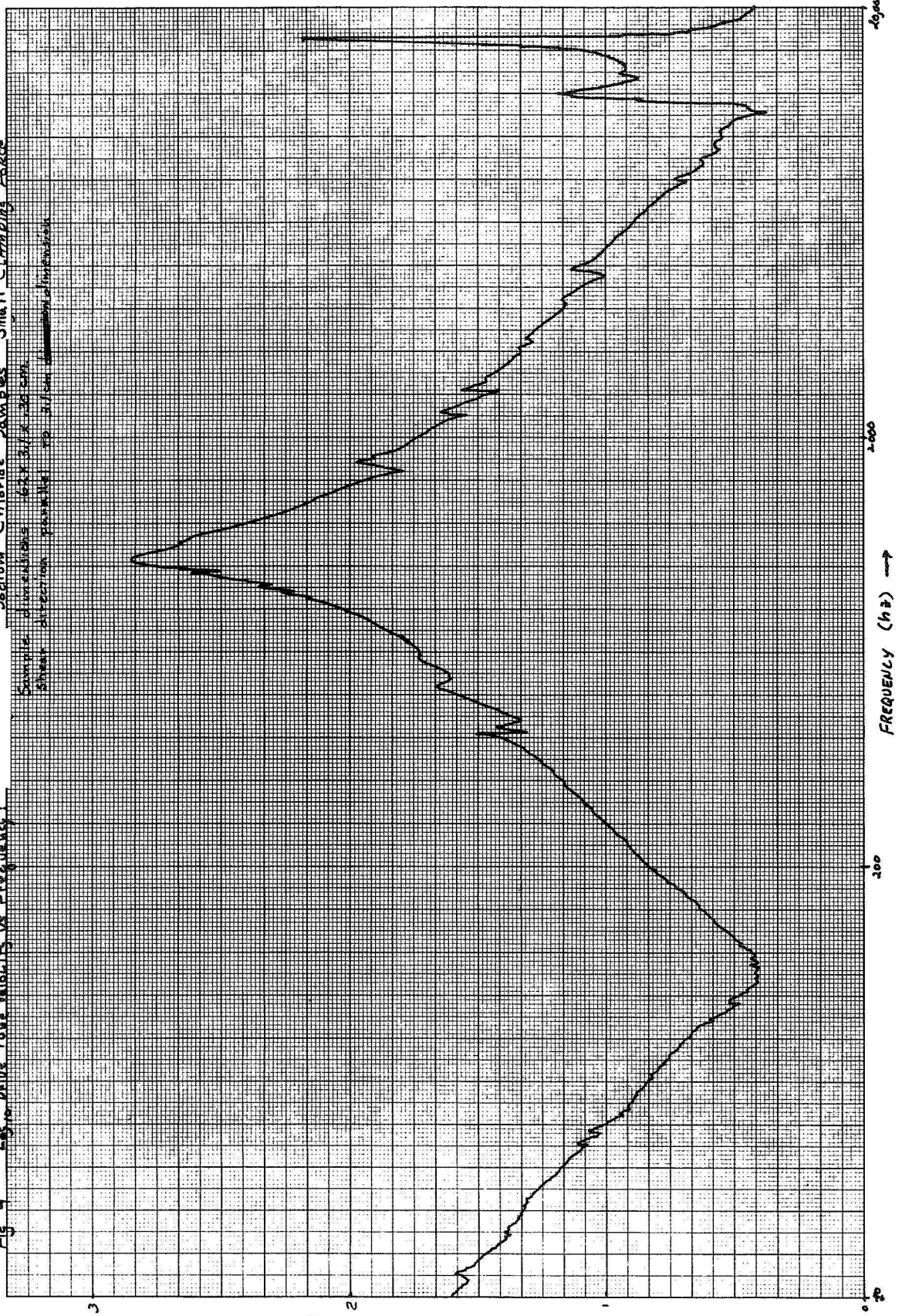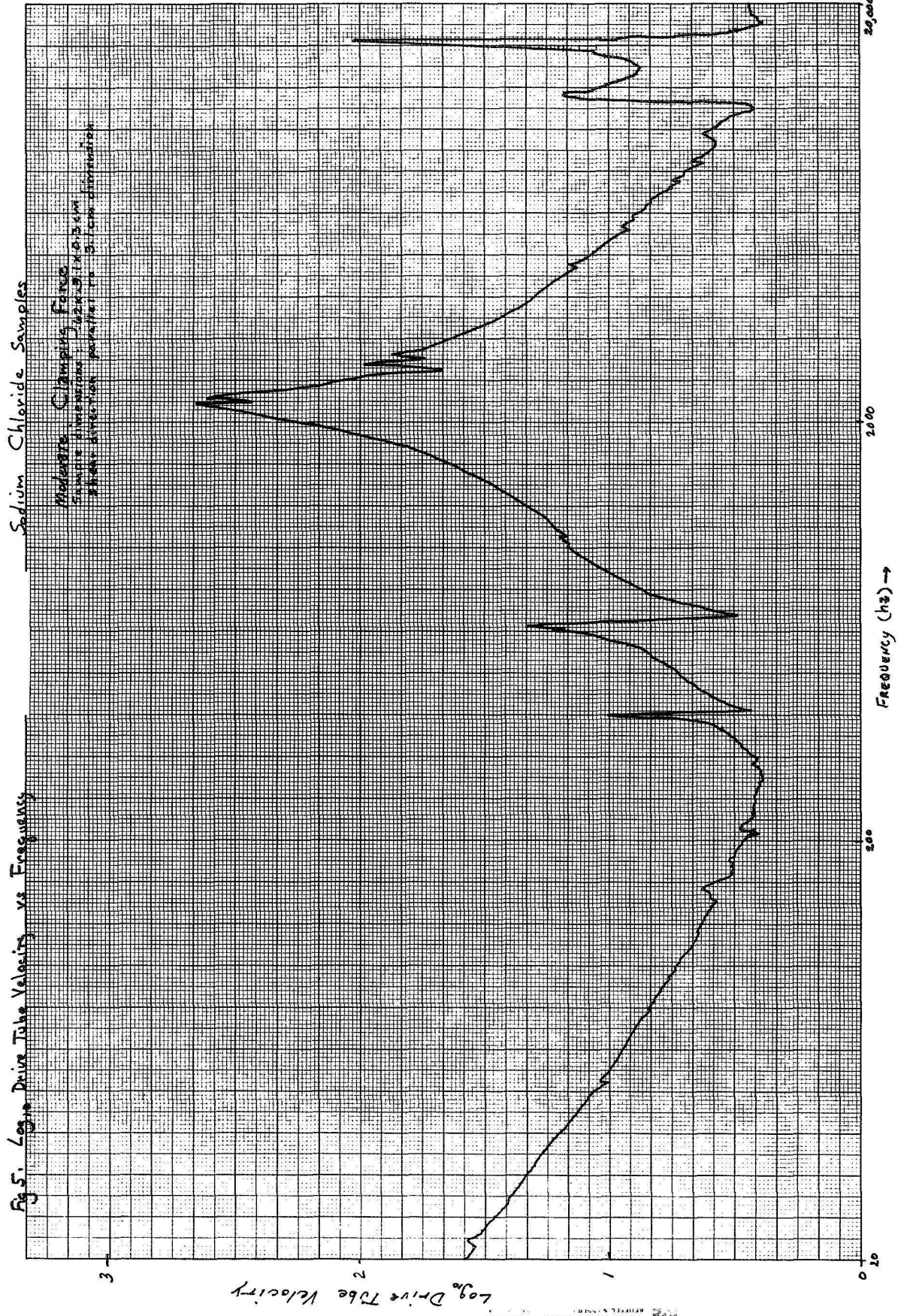
FREQUENCY (Hz) →

Log₁₀ Drive Tube Velocity

Fig. 8   Log₁₀ Drive Tube Velocity vs Frequency

Sodium Chloride Samples

Clamping Force = 111 x 10⁵ dynes
Sample dimensions: 0.8 x 0.8 x 0.2 cm
Shear attenuation plotted in db/in dimensions
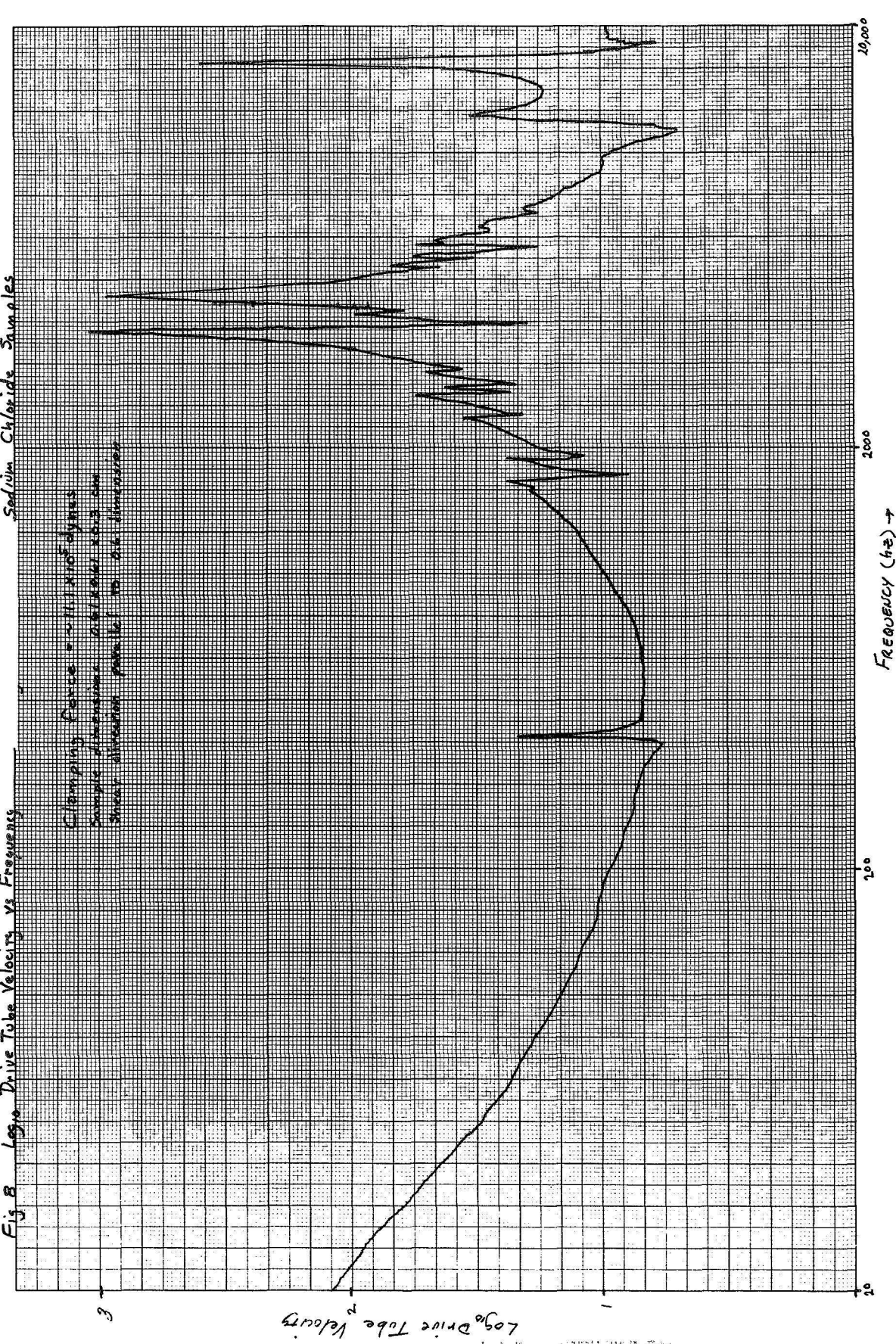
Frequency (hz) →

Fig. 9. Log_{10} Drive Tube Velocity vs. Frequency: Sodium Chloride Samples

Clamping force = applied 5 x 10⁵ dynes
Sample dimensions ...
Shear direction parallel to axal dimension

Frequency (Hz) →

Log_{10} Drive Tube Velocity

3   2   1   0

200   2000   20,000   10

Portion of Aluminum
Drive tube near
Pole Piece.

Central
Magnetic Pole Piece

Lucite Disk

Air Gap
of Magnet

Aluminum Foil
Cemented to
Lucite Disk
(Right Probe)

300 volts

R

L

B
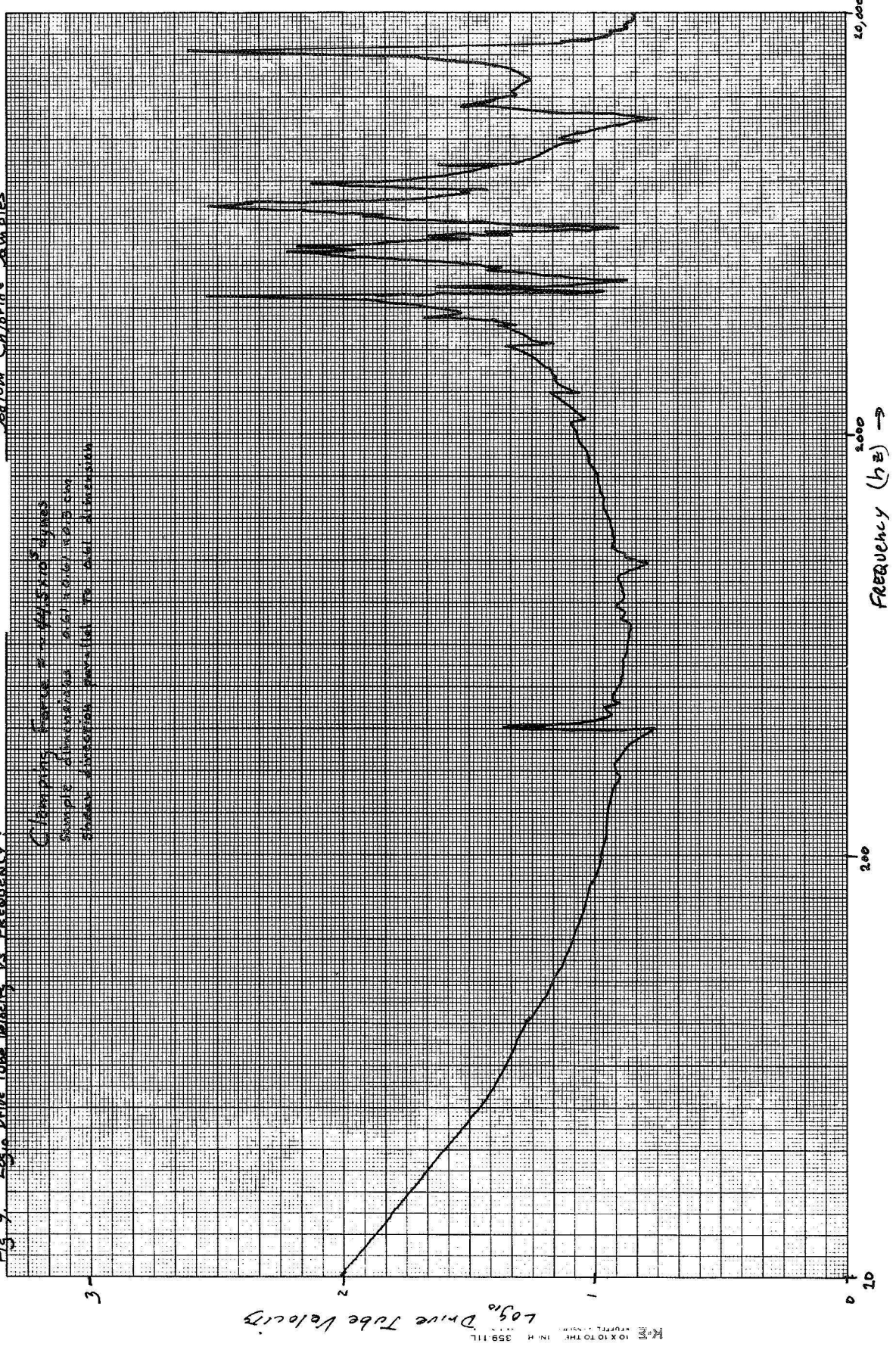
Aluminum Foil
Cemented to Lucite
Disk
(Left Probe)

Aluminum Foil
Cemented to Lucite Disk
(Bottom probe)
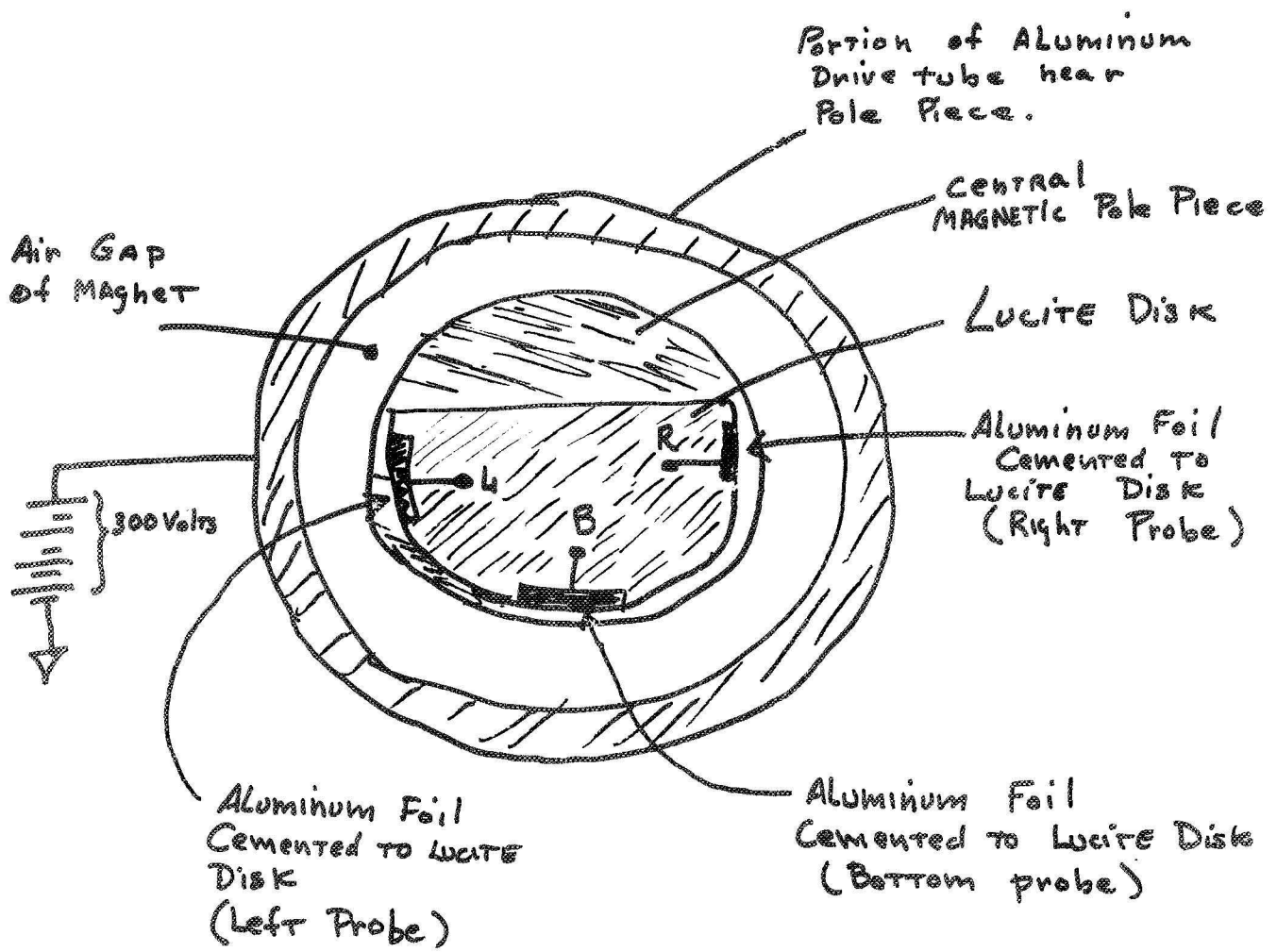
Fig 10. Capacitance Probe System:

Three Aluminum foils (left, right and bottom)
are capacitively coupled to aluminum drive tube which
is held at 300 volts above ground. Radial displacement
of the drive tube ~~is~~ induces ~~voltage~~ current flow
in a high impedance Amplifier connected to Terminals L, B or R.

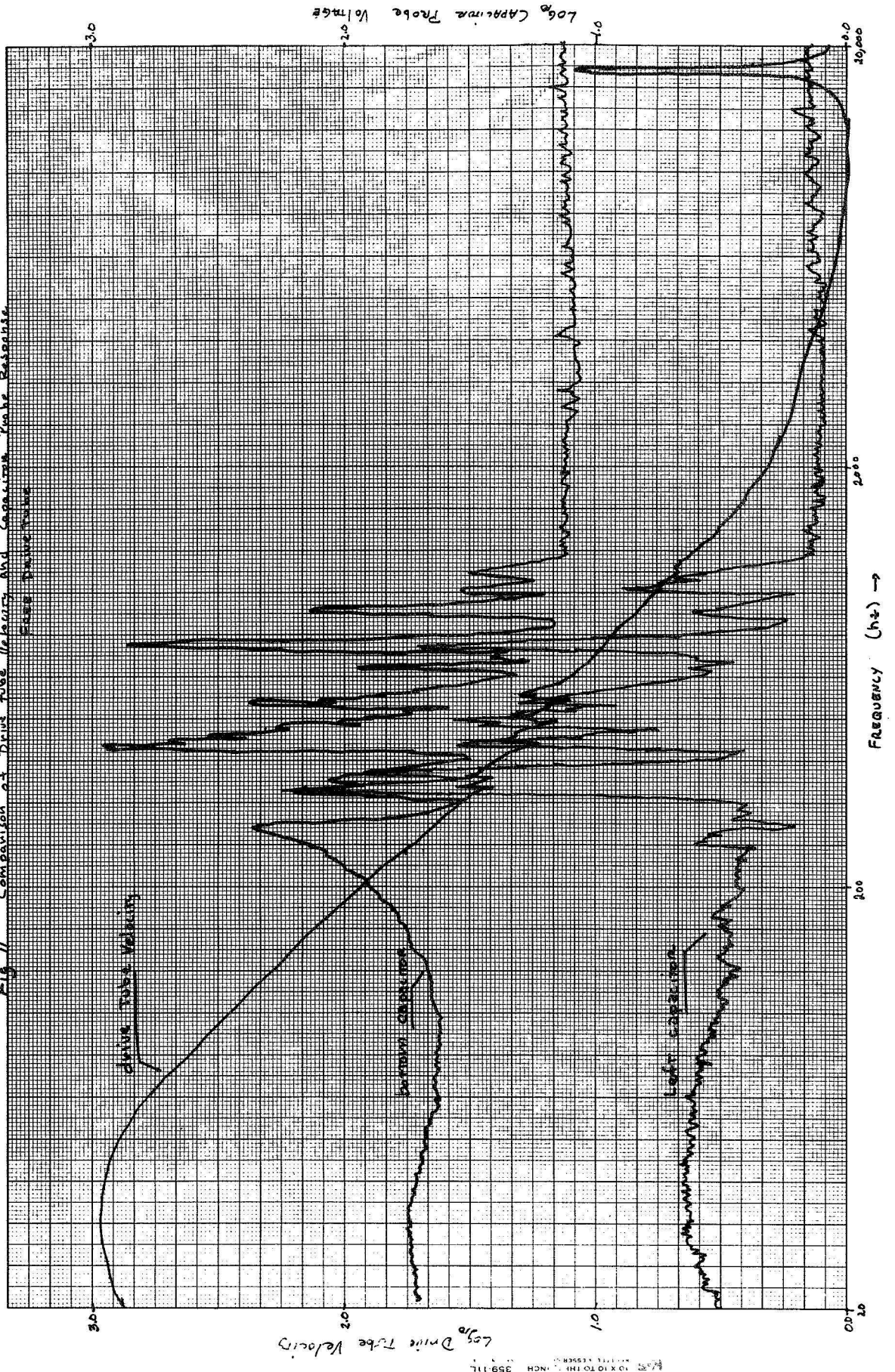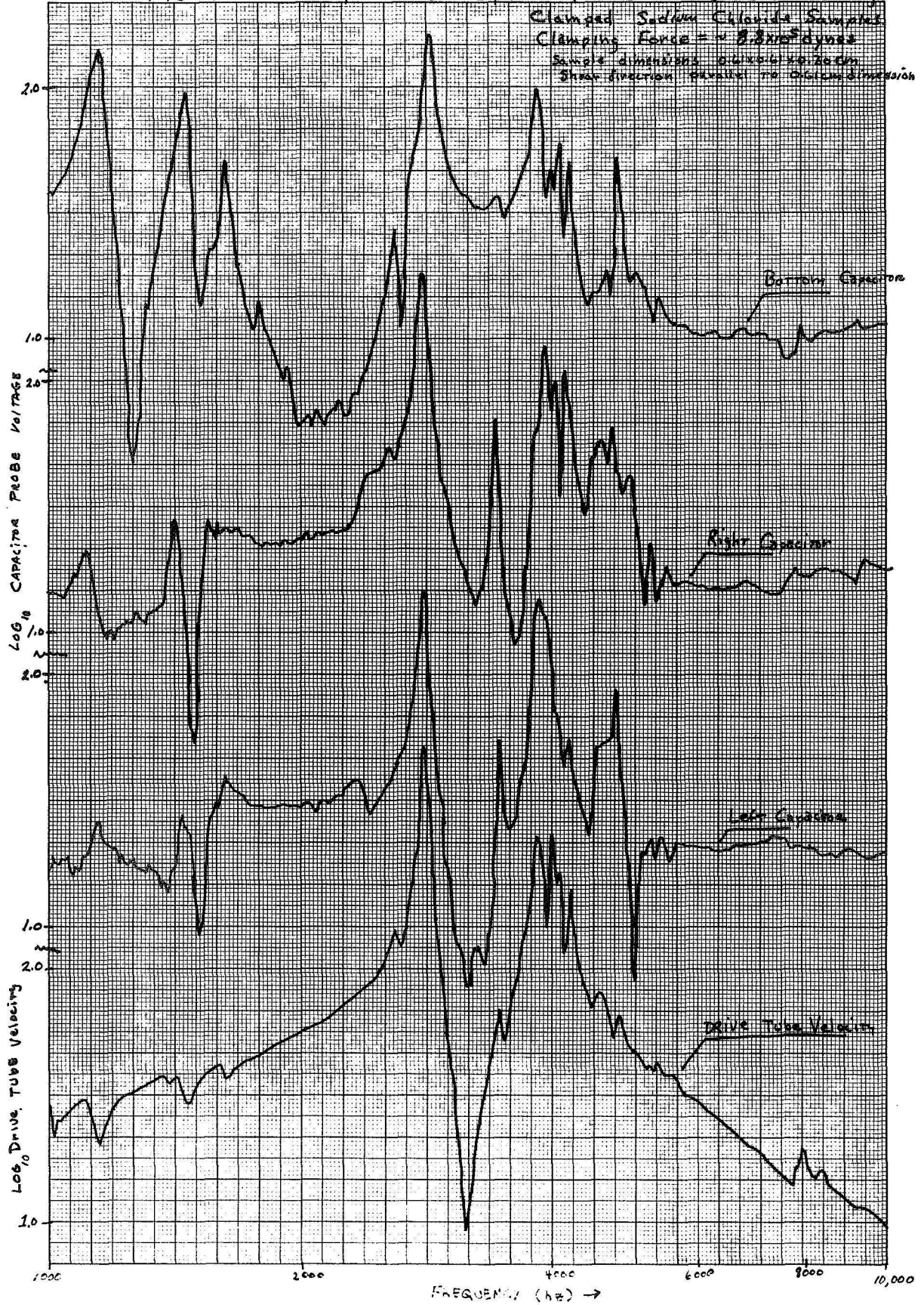Fig 11 Comparison of Drive Tube Velocity and Capacitive Probe Response

FIG 12. Comparison of Capacitor Probes with Drivetube Velocity

Clamped Sodium Chloride Samples
Clamping Force = ~ 3.8×10⁵ dynes
Sample dimensions 0.61×0.61×0.20 cm
Shear direction parallel to 0.61cm dimension

Bottom Capacitor

Right Capacitor

Left Capacitor

Drive Tube Velocity

LOG₁₀ CAPACITOR PROBE VOLTAGE

LOG₁₀ DRIVE TUBE VELOCITY

FREQUENCY (hz) →

1,000   2,000   4,000   6,000   8,000   10,000
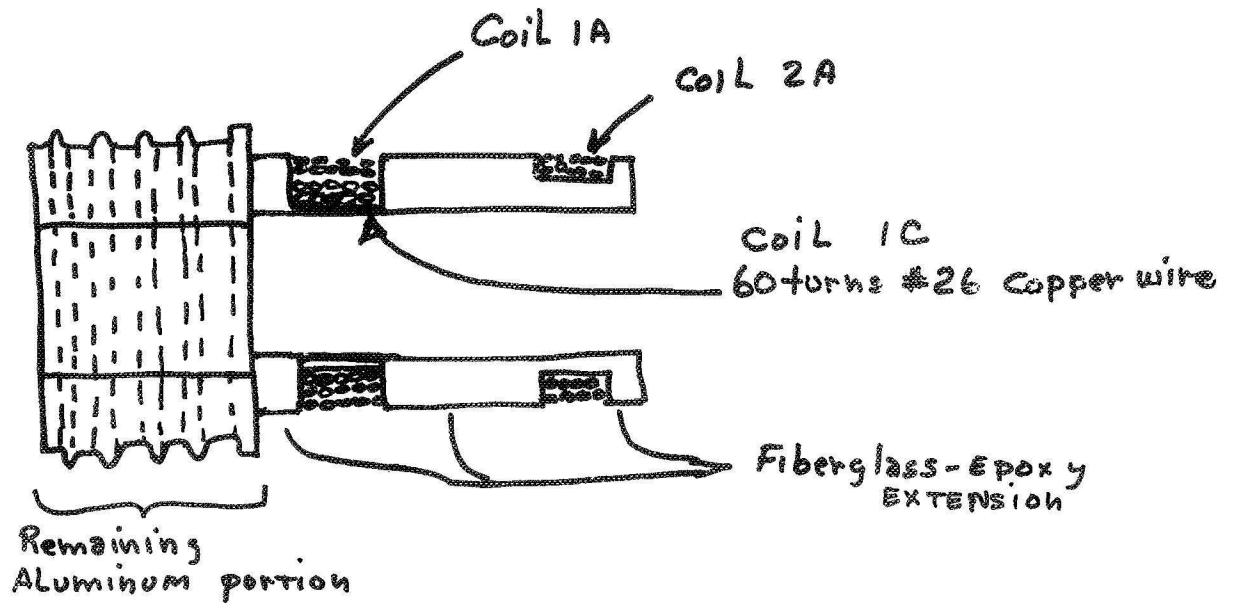
Figure 13.

Modified Drive tube with Fiberglass extension showing coil 1c which is used to simulate the shorted turn of Fitzgerald's design.

Fig. 14

Comparison of Drive Tube Velocity

Fast Error (instantaneous) Drive Tube
with coil in open-circuited and close-circuited
conditions

open-circuited coil in

close circuited
coil in
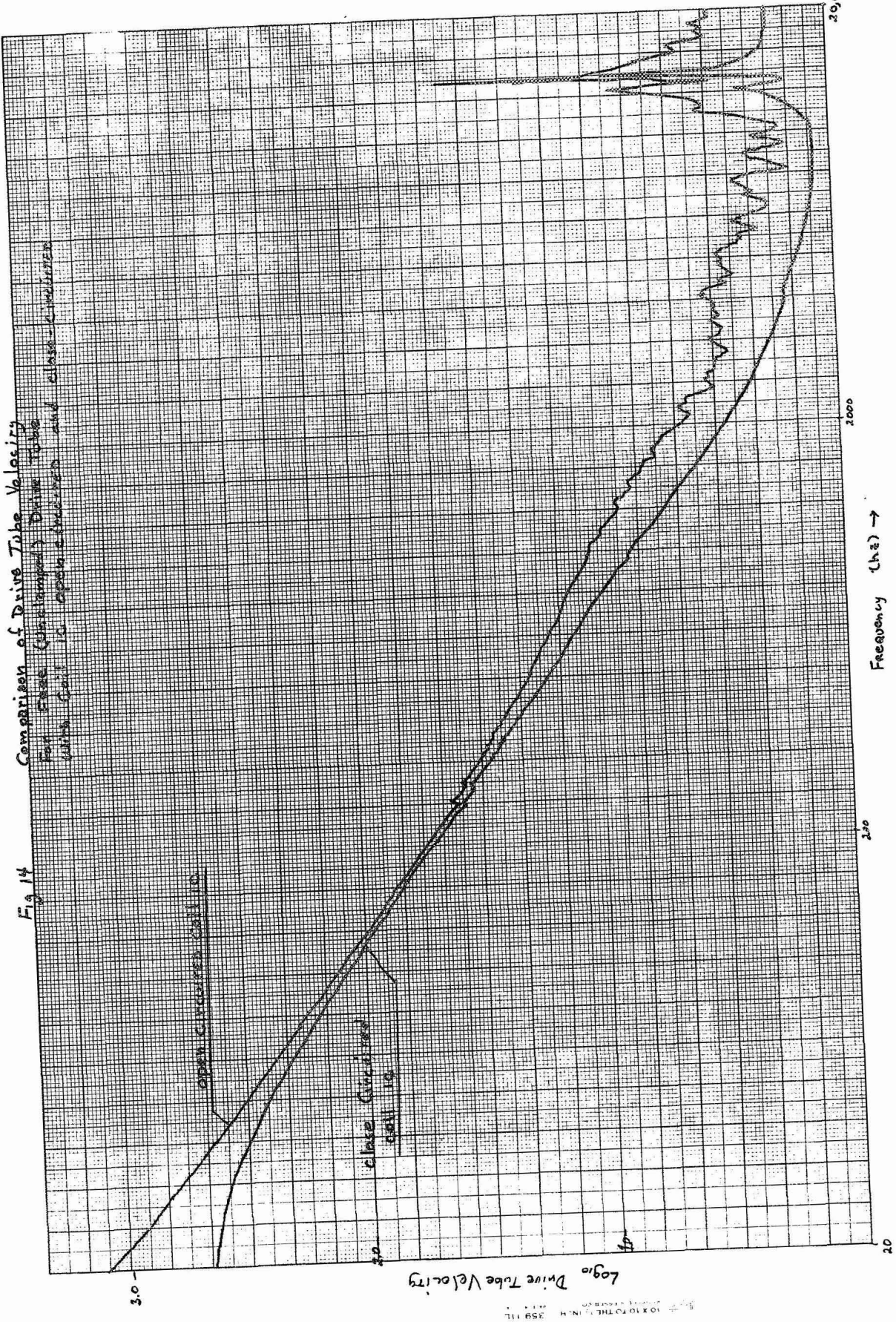
Log₁₀ Drive Tube Velocity

Frequency (Hz) →

Fig 15   Comparison of Drive Tube Velocity For open and close-circuit Coil Ic

Sodium Chloride Samples .68×.61×.3 cm.
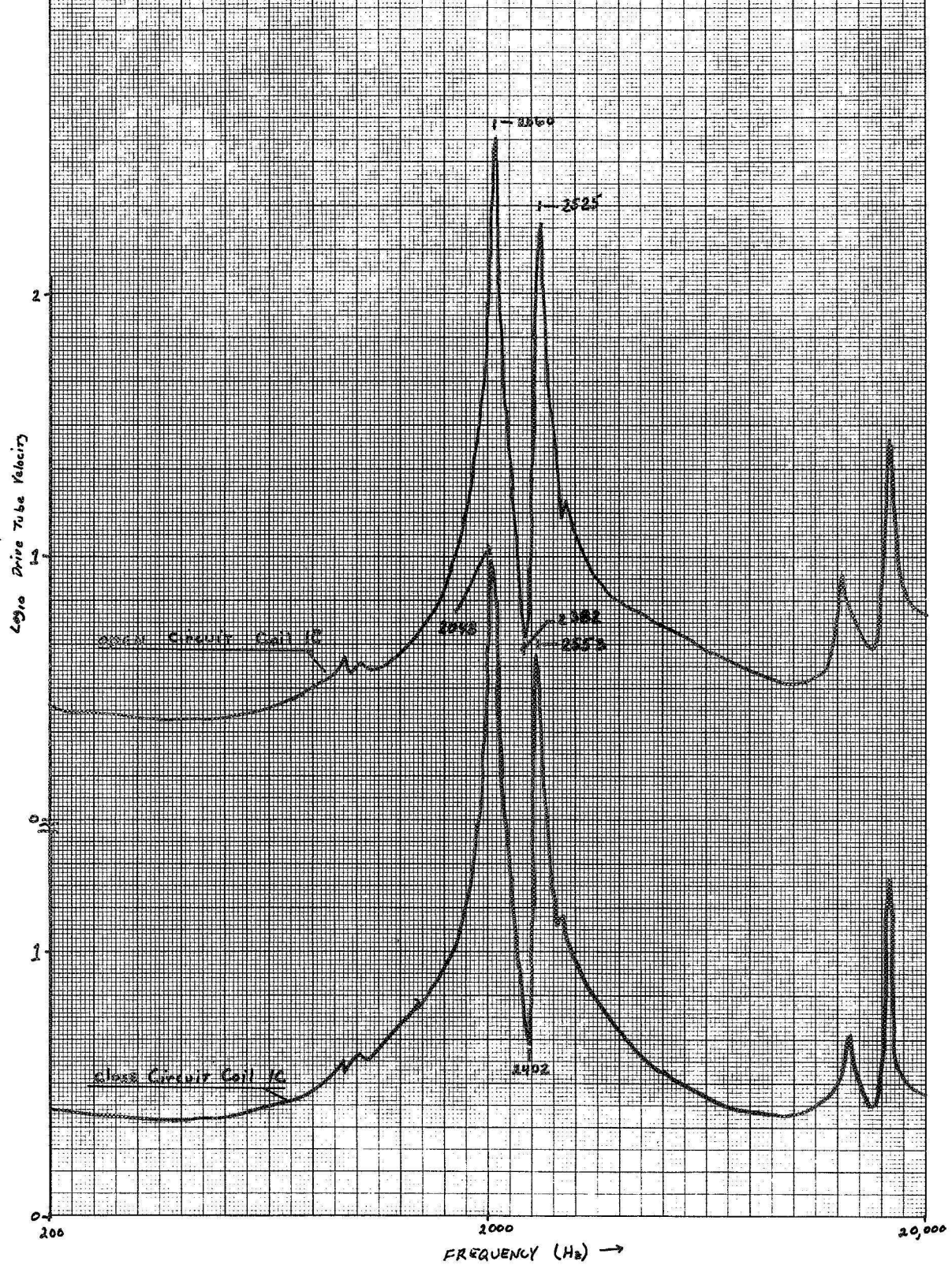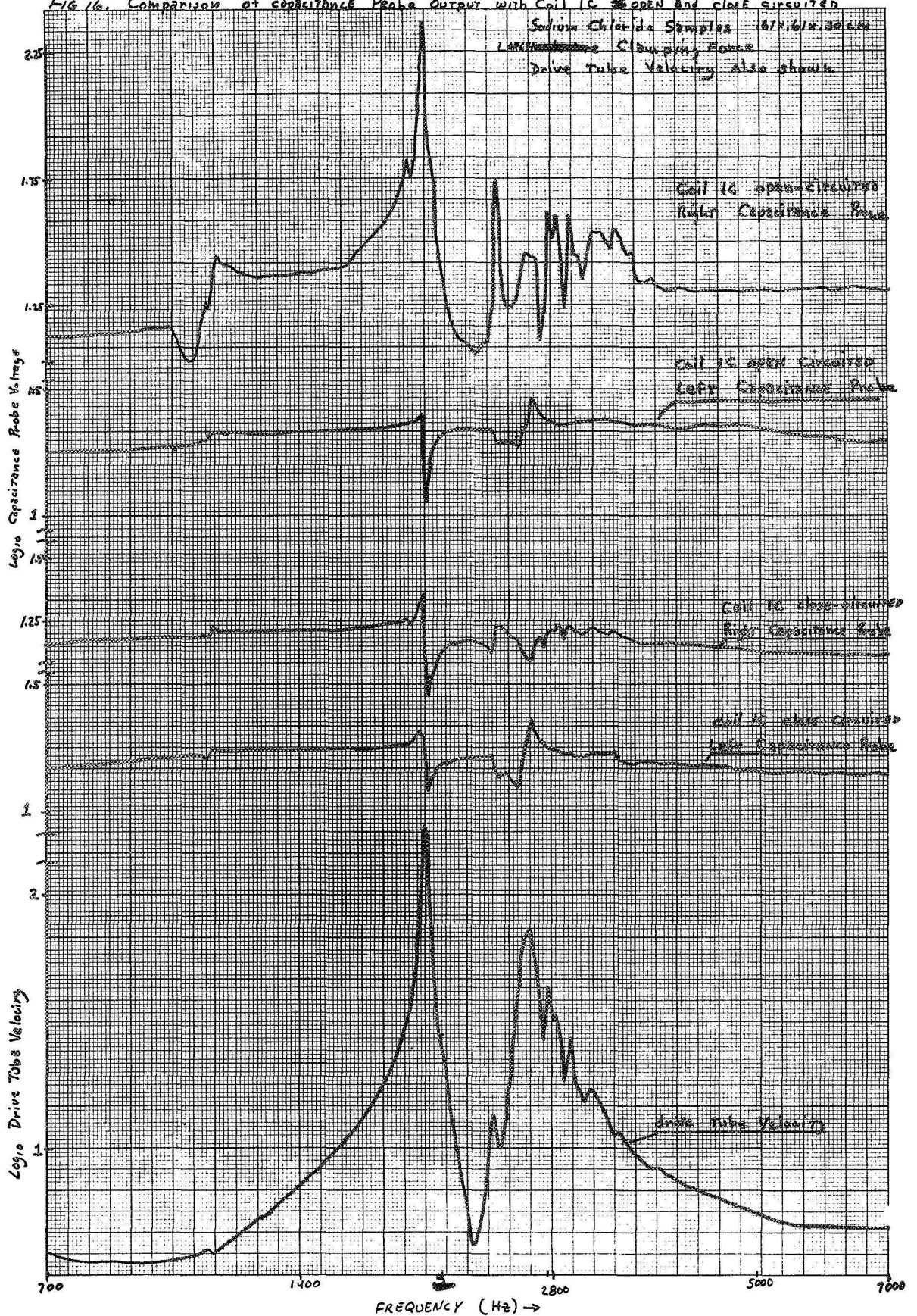
Measure Clamping Force

FREQUENCY oF EXTREMUM INDICATED

FIG 16. Comparison of capacitance Probe Output with Coil IC Open and close circuited

Sodium Chloride Samples 15/16×15/16×30 cms
Large Clamping Force
Drive Tube Velocity also shown

Coil IC open-circuited
Right Capacitance Probe

Coil IC open circuited
Left Capacitance Probe

Coil IC close-circuited
Right Capacitance Probe

Coil IC close-circuited
Left Capacitance Probe

drive Tube Velocity

Log₁₀ Capacitance Probe Voltage

Log₁₀ Drive Tube Velocity

FREQUENCY (Hz) →
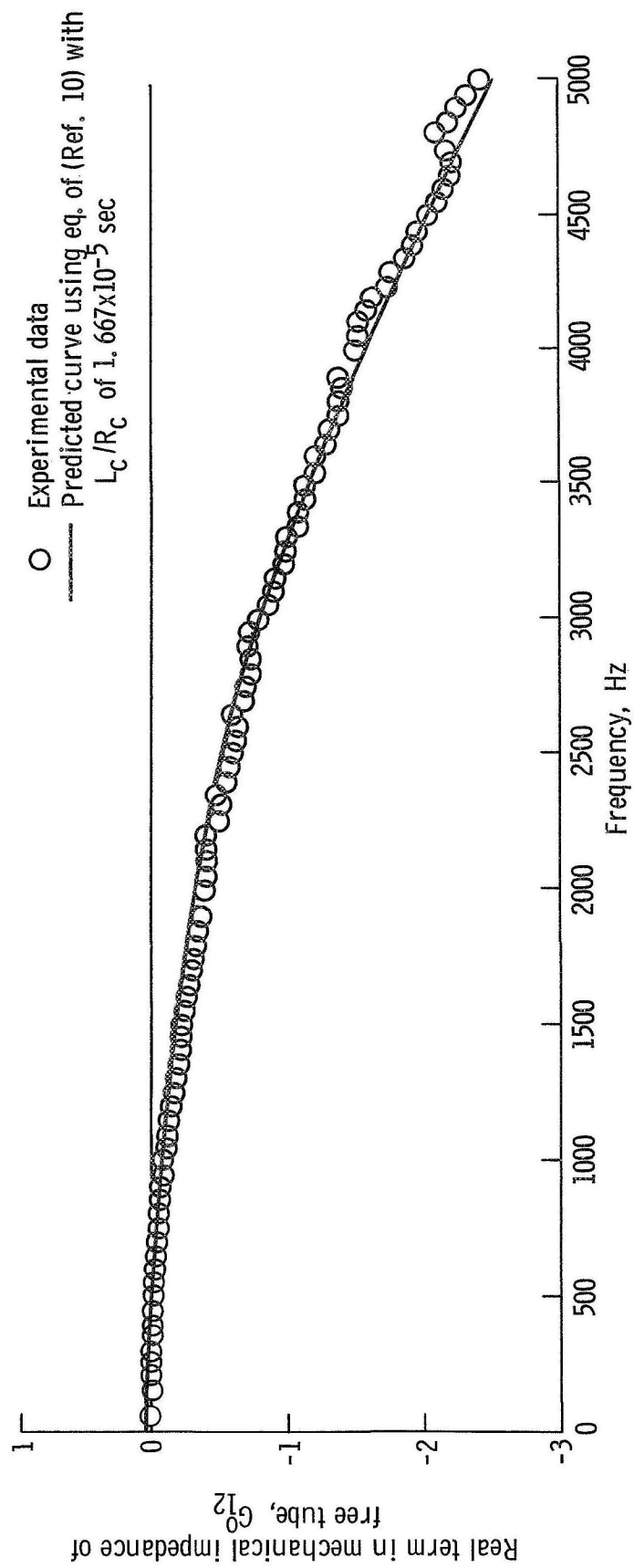
700   1400   2800   5000   7000

Figure 17. – Comparison of experimental calibration data of real term in mechanical impedance of free tube with that calculated using shorted drive tube analysis (Ref. 10).

Fig 1B. FREE Tube Calibration Data G°₁₂ vs Frequency

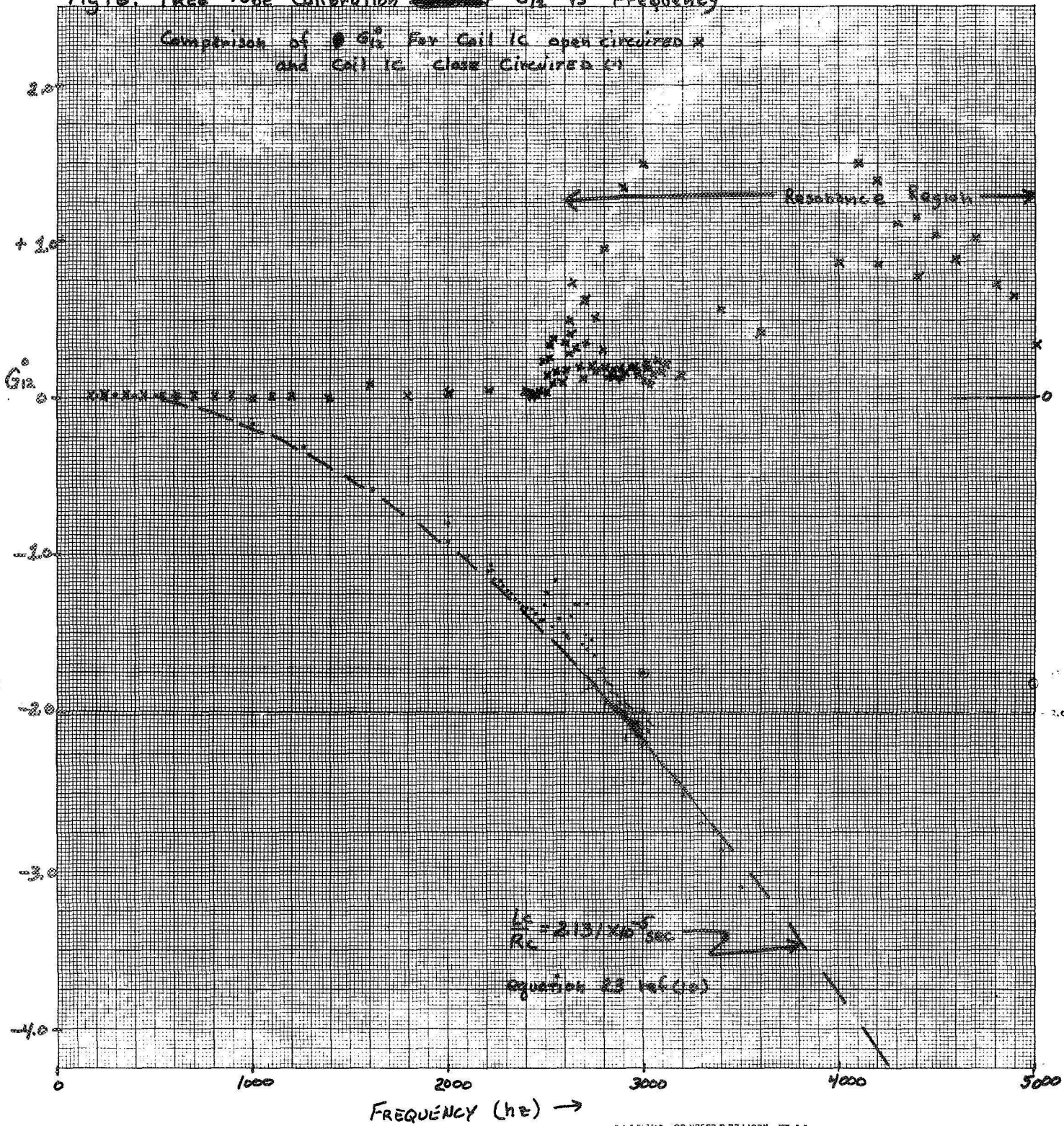Comparison of G°₁₂ For Coil IC open circuited x
and Coil IC close circuited (·)

$$\frac{L_c}{R_c} = 2.131 \times 10^{-5} \text{ sec}$$
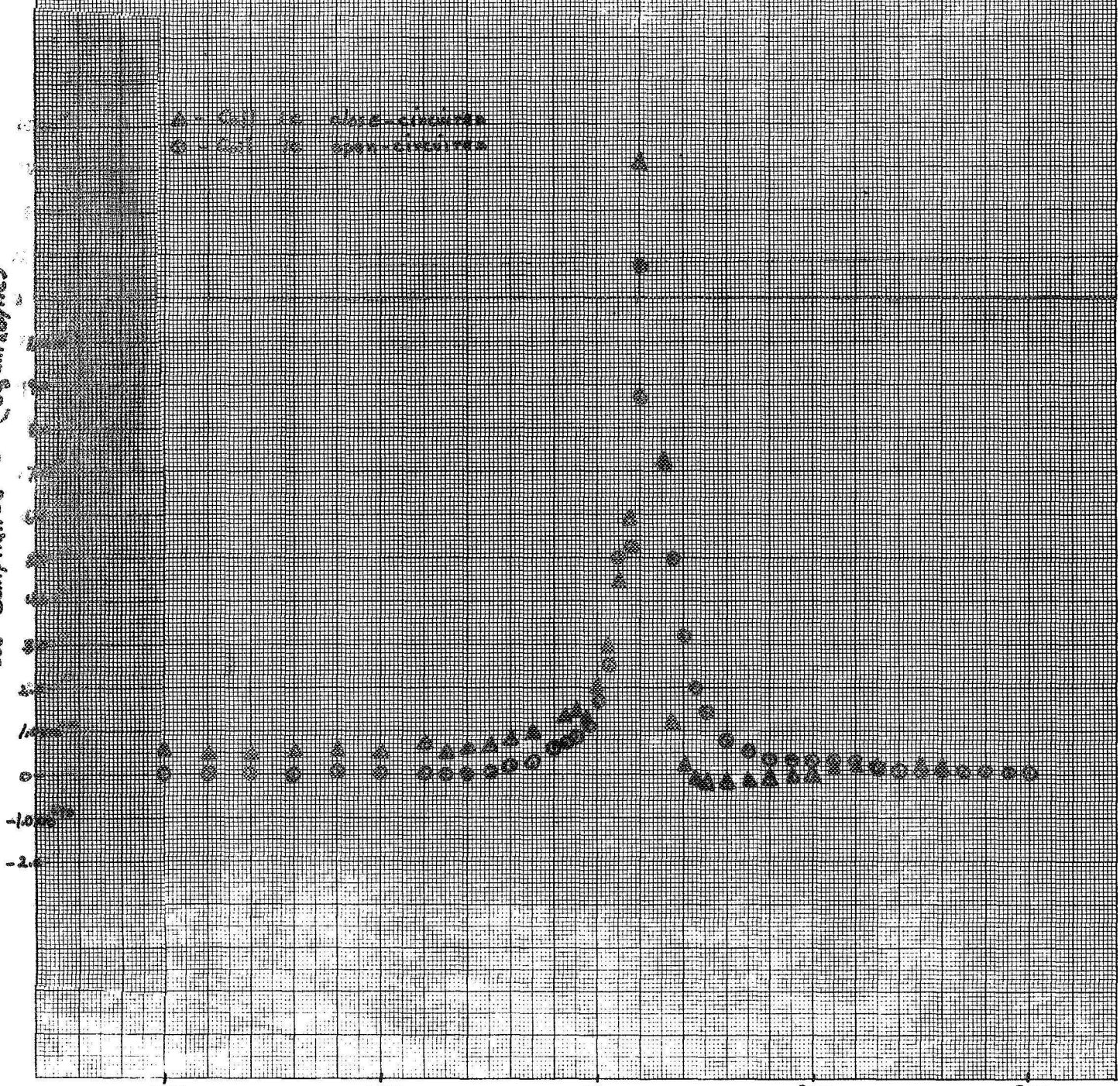
Equation 23 Ref (20)

FREQUENCY (hz) →

Fig. 14   Comparison of Loss Compliance Values vs. Frequency
for data obtained with Coil to close circuit and open circuit
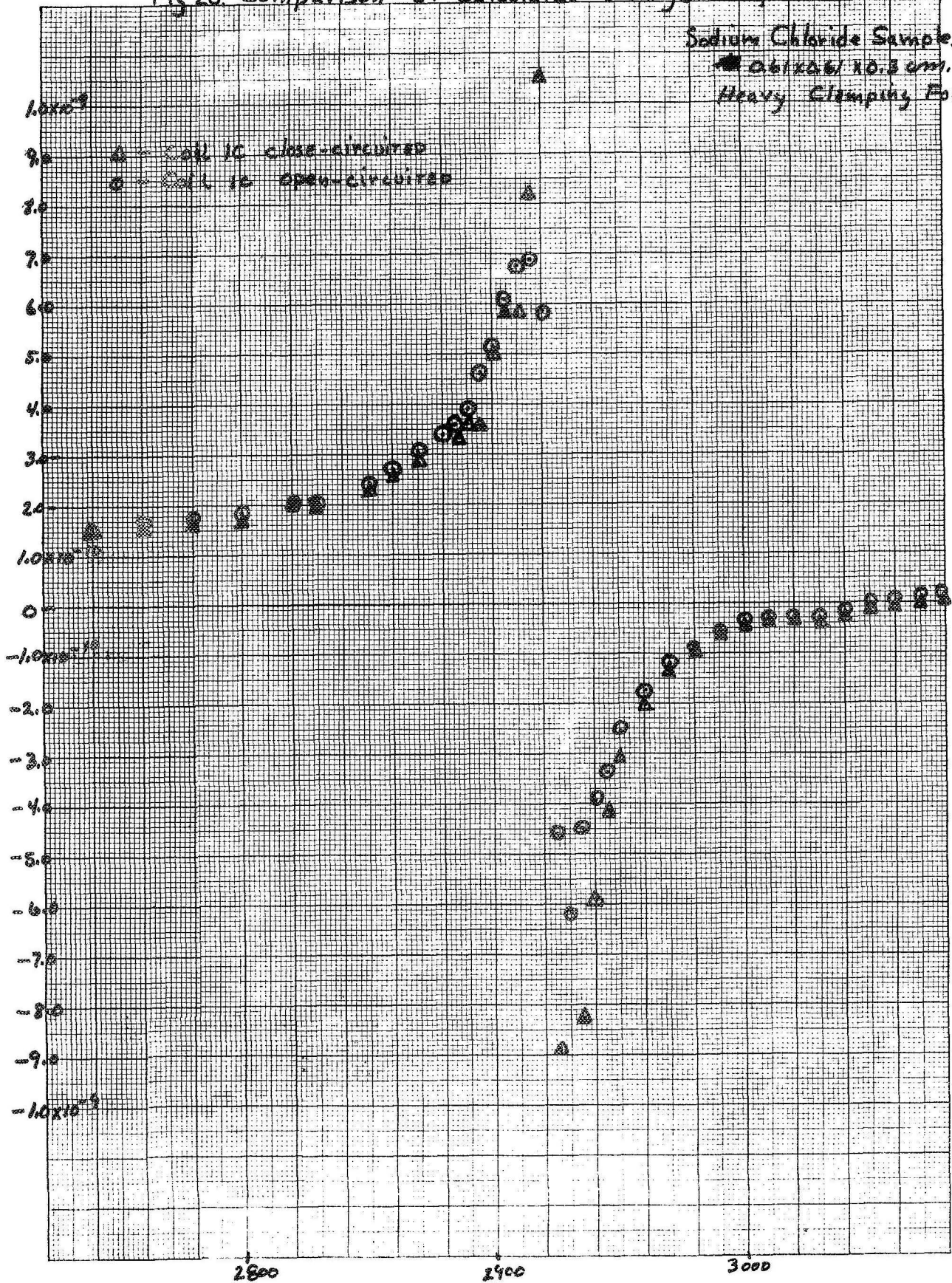Sodium Chloride Sample   [illegible]
Heavy Clamping force

△ — Coil to close-circuit
○ — Coil to open-circuit

Loss Compliance S'' (Sq cm/dyne)

Frequency (Hz) →

Fig 20. Comparison of Calculated Storage Compliance J' vs Frequency

Sodium Chloride Samples
0.61 × 0.61 × 0.3 cm.
Heavy Clamping Force

△ = cell IC close-circuited
○ = cell IC open-circuited